American Mineralogist, Volume 84, pages 1439–1444, 1999

Parascorodite, $FeAsO_4 \cdot 2H_2O$—a new mineral from Kaňk near Kutná Hora, Czech Republic

PETR ONDRUŠ,[1,*] ROMAN SKÁLA,[1] CECILIA VITI,[2] FRANTIŠEK VESELOVSKÝ,[1] FRANTIŠEK NOVÁK,[3] AND JIŘÍ JANSA[3]

[1]Czech Geological Survey, Klárov 3/131, P.O. Box 85, CZ-118 21 Prague 1, Czech Republic
[2]Dipartimento di Scienze della Terra, Via Laterina, 8, I-53100 Siena, Italy
[3]Institute of Raw Materials, CZ-284 03 Kutná Hora 425, Czech Republic

ABSTRACT

Parascorodite, a new mineral from Kaňk near Kutná Hora, Central Bohemia, Czech Republic, forms earthy white to white-yellow aggregates associated with scorodite, pitticite, bukovskýite, kaňkite, zýkaite, gypsum, and jarosite, wet chemical analysis gave (in wt%): As_2O_5 44.45, P_2O_5 0.84, SO_3 1.53, Fe_2O_3 34.55, Al_2O_3 0.17, H_2O 17.81, totaling 99.95. The simplified chemical formula is $FeAsO_4 \cdot 2H_2O$. Selected area electron diffraction suggests hexagonal or trigonal symmetry. The extinction symbol is *P-c-*. Powder X-ray diffraction yielded unit-cell parameters a = 8.9327(5) Å, c = 9.9391(8) Å, V = 686.83 (8) Å^3, Z = 6. Densities (measured and calculated, respectively) are D_m = 3.213(3) g/cm^3 and D_x = 3.212 g/cm^3. SEM and TEM images showed that basal sections of parascorodite are hexagonal in shape; thicker prismatic crystals were also observed. Crystal size varies between 0.1 to 0.5 µm. The strongest lines in the X-ray powder diffraction pattern are [*d*[I](*hkl*)]: 4.184(44)(012), 4.076(100)(111), 3.053(67)(202), 2.806(68)(211), 2.661(59)(113), 2.520(54)(212), 2.2891(44)(032). Refractive indexes could not have been measured due to extremely small crystallite size, $\overline{n}$ (calc) = 1.797. The TG curve shows two weight losses: at 20–150 °C (2.1 wt%, absorbed water) and at 150–620 °C (15.5 wt%, molecular water), respectively. They correspond to the endothermic peaks on the DTA curve at 120 and 260 °C. Strong exothermic reaction observed at 585 °C reflects formation of the phase $FeAsO_4$. Infrared absorption spectra of parascorodite are close to those of scorodite.

INTRODUCTION

Parascorodite was first identified in 1967 by X-ray powder diffraction methods as an unknown admixture in massive pale green-gray scorodite associated with bukovskýite on medieval dumps of the Kaňk mine near Kutná Hora. In 1974, this phase was found as earthy aggregates in porous masses of kaňkite. Only new finds of parascorodite and recent development of sophisticated experimental methods has allowed formal description of this mineral.

The holotype material is deposited in the mineralogical collection of the National Museum, Prague, Czech Republic (the acquisition number P1p 25/98). The new mineral and its name were approved by the Commission on New Mineral and Mineral Names of IMA.

OCCURRENCE AND PARAGENESIS

Parascorodite is one of the rarest secondary minerals found at Kaňk in the Kutná Hora ore district (Central Bohemia, Czech Republic) from heavily weathered ore dumps (Kuntery mine) that date from the period when the ore district was a major source of silver and polymetallic ores. The dumps probably represent arsenic rich ore which, in medieval times, were considered mine waste. There are distinct relics of arsenopyrite in vein quartz-pyrite-arsenopyrite material of the dumps, and we assume that majority of secondary iron arsenates and arsenosulfates did not originate after disposal of the material on dumps, but formed much earlier as products of natural weathering in the supergene zone of the deposit. Parascorodite represents one of the youngest iron arsenates at Kaňk, being most frequently associated with earthy scorodite and pitticite. Other associated minerals are bukovskýite, kaňkite, zýkaite, gypsum, jarosite and amorphous ferric hydroxides (Trdlička and Hoffman 1965, Novák et al. 1967, Čech et al. 1976, 1978).

Ondruš et al. (1997a, 1997b, 1997c) identified parascorodite in the Geschieber vein of the Svornost mine in the Jáchymov (Joachimsthal ore district), where it is associated with scorodite in quartz gangue, with pyrite, proustite and small spherical aggregates of kaňkite. The aggregates occur in small cavities of quartz gangue. Parascorodite is associated there with vajdakite $(Mo^{6+}O_2)_2As^{3+}_2O_5 \cdot 3H_2O$ and native arsenic (Ondruš et al. 1997a, 1997c).

Parascorodite is apparently a product of arsenopyrite dissolution, followed by later re-crystallization of iron-arsenic-bearing solutions in conditions of subrecent-to-recent near-surface weathering. Parascorodite is dimorphous with

*E-mail:ondrus@cgu.cz

scorodite, which is its most common companion. It obviously forms only as a transitional metastable phase during formation of iron arsenates at very specific conditions of supergene zone, favorable for its preservation.

PHYSICAL PROPERTIES

At Kaňk, parascorodite occurs as earthy, soft cryptocrystalline aggregates of poorly developed hemispherical shape. The aggregates are white with a yellowish tint and yellowish-white streak, they are up to 2 cm across, and consist of extremely small crystals often arranged in fan-like or irregular masses (Fig. 1). Crystal size varies between 0.1 to 0.5 μm; exceptionally, twinned individuals up to 1 μm were observed by TEM. Crystals occur as prisms or thin flakes (probably due to parting) of hexagonal outline (Fig. 2). The measured density of earthy aggregates by weighing in ethylalcohol is 3.213(3) g/cm^3 and the calculated density (for $Z = 6$) is 3.212 g/cm^3. At Jáchymov, parascorodite occurs always in a mixture with scorodite (orthorhombic $Fe^{3+}AsO_4 \cdot 2H_2O$) in very rare, white or greenish gray, earthy aggregates with a conchoidal fracture.

Parascorodite dissolves slowly in 10% HCl, but no reaction with water was observed. However, earthy aggregates disintegrate relatively rapidly into powder. Under hydrothermal conditions (distilled water, sealed quartz glass container, temperature of 155 °C) lasting for a period of two months, parascorodite re-crystallizes to scorodite.

In transmitted light, parascorodite aggregates are very pale yellow to brown, and are undistinguishable from scorodite. Refractive indexes could not be measured because of extremely small crystal size. When observed in CH_2I_2, aggregates of parascorodite display a mean refractive index higher than 1.72 and very low to almost indiscernible birefringence. The mean refractive index, calculated from Gladstone-Dale rule, is 1.797.

TABLE 1. Chemical analyses of parascorodite (wt%) from Kaňk

	1	2	3
As_2O_5	44.45	44.37–44.53	49.79
P_2O_5	0.84	0.62–1.06	
SO_3	1.53	1.50–1.56	
Fe_2O_3	34.55	34.42–34.68	34.59
Al_2O_3	0.17	0.11–0.23	
H_2O^+	16.81	16.50–17.12	15.61
H_2O^-	1.60	1.44–1.76	
Total	99.95		

Note: 1 = average of two wet chemical analyses; 2 = range of two analyses; 3 = ideal composition required by formula $FeAsO_4 \cdot 2H_2O$.

CHEMICAL COMPOSITION

Qualitative spectral chemical analysis of parascorodite indicated two major elements only—iron and arsenic. Other elements (Cu, Zn, Sn) were below 0.X wt%. Quantitative chemical composition was determined from two wet chemical analyses and a thermal analysis (Table 1). The empirical formula of parascorodite, based on six oxygen atoms per formula unit, is

$Fe^{3+}_{0.979}Al_{0.007}[(AsO_4)_{0.875}(PO_4)_{0.027}(SO_4)_{0.043}(OH)_{0.166}] \cdot 2.05H_2O$,

resulting in the simplified formula $FeAsO_4 \cdot 2H_2O$.

THERMAL DATA

Thermogravimetry (TG), differential thermal analysis (DTA), and differential thermogravimetric (DTG) curves (Fig. 3) were recorded simultaneously on a theromogravimeter Derivatograph Q-1500 D (MOM Budapest). The operation conditions were as follows: sample weight 560 mg, heating rate 10 °C/min, and temperature range 20–950 °C. Three ranges of weight loss can be identified on the TG-curve. The first interval (20–150 °C) has a barely detectable loss maximum at about 100 °C. The loss of 2.1 wt% corresponds to absorbed water. This is correlated with a very weak endothermic reaction occurs at 120 °C on the DTA curve. The second interval (150–620 °C) has a

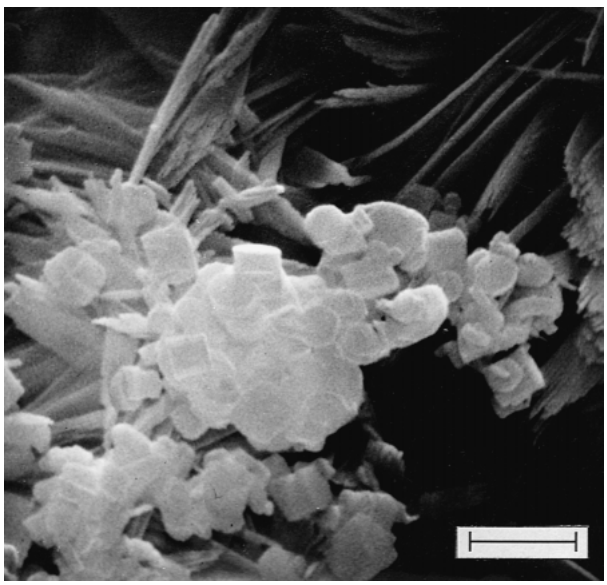

FIGURE 1. Scanning electron micrograph of the aggregate of parascorodite crystals; scale bar corresponds to 2 μm.

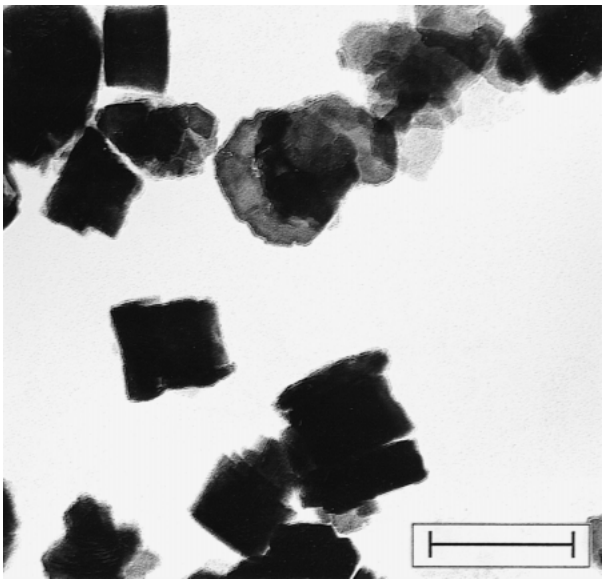

FIGURE 2. A TEM image of parascorodite crystals, note hexagonal thin flakes and thick prisms of this mineral; scale bar corresponds to 590 nm.

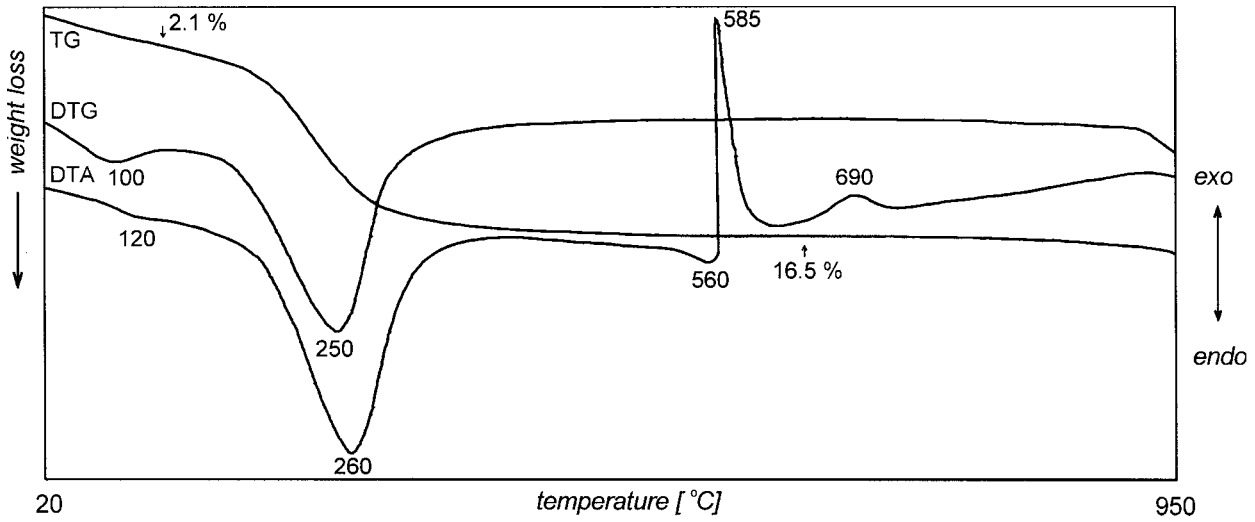

FIGURE 3. Differential thermal analysis (DTA), thermogravimetric (TG) and differential thermogravimetric (DTG) curves for parascorodite.

maximum weight loss at 260 °C, corresponding to the escape of molecular water amounting to 15.5 wt%. A very strong endothermic reaction was observed on the DTA curve at 260 °C. Third, a slow decrease in weight loss occurs above 620 °C caused by decomposition of the phase $FeAsO_4$ (d'Yvoire et al. 1968), which forms by very strong exothermic re-crystallization observed at 580 °C. Fourth, one additional weak exothermic reaction at 690 °C reflects formation of the phase $FeAsO_4$(I) (d'Yvoire et al. 1968). This phase was confirmed by X-ray diffraction of the end-product of parascorodite heating (at 950 °C). Parascorodite did not change its crystal structure when heated to 120 °C for one hour. Upon heating to 1400 °C, only α-Fe_2O_3 was confirmed by X-ray diffraction.

X-RAY POWDER DIFFRACTION DATA

An XRD pattern of parascorodite was collected using a Philips X'pert MPD System (Cu radiation, graphite secondary monochromator 40 kV, 40 mA, range 2θ = 3–70°, step in 2θ = 0.01°, time = 10 s). Data were processed using the ZDS-system software, version 6.01 (Ondruš and Skála, in preparation). Lanthanum hexaboride mixed with metallic silicon was used as an external standard.

The parascorodite unit cell inferred below is hexagonal or trigonal, with extinction symbol *P-c-*. Unit-cell parameters refined from the powder data (Table 2) are a = 8.9327(5) Å, c = 9.9391(8) Å, volume V = 686.83 (8) Å^3, axial parameter ratio $c:a$ = 1.1127:1, and number of formula units per unit cell Z = 6.

TRANSMISSION ELECTRON MICROSCOPY AND SELECTED AREA ELECTRON DIFFRACTION

Parascorodite samples are unsuitable for classic XRD single-crystal structure study because the grain size is well below resolution of an optical microscope. To prove parascorodite symmetry and unit cell dimensions, a transmission electron microscopy (TEM) was used.

A TEM analysis was done on a Philips 400T analytical microscope, working at 120 kV. A 50 μm objective aperture was used for the image formation, with a corresponding nominal point-to-point resolution close to 4 Å. The selected area aperture to obtain diffraction patterns (selected-area electron-diffraction, SAED) was approximately 0.5 μm in diameter. Parascorodite powder was dispersed in double distilled water and deposited on two Cu mesh grids, previously covered by a graphite film (support). The grids with the experimental charge were then covered by a graphite film (cover).

Euhedral to subhedral crystals of parascorodite were observed as either thicker prisms or thin flakes—the latter displayed distinct hexagonal outline. Prismatic crystals show very straight boundaries, while thin hexagonal flakes frequently have

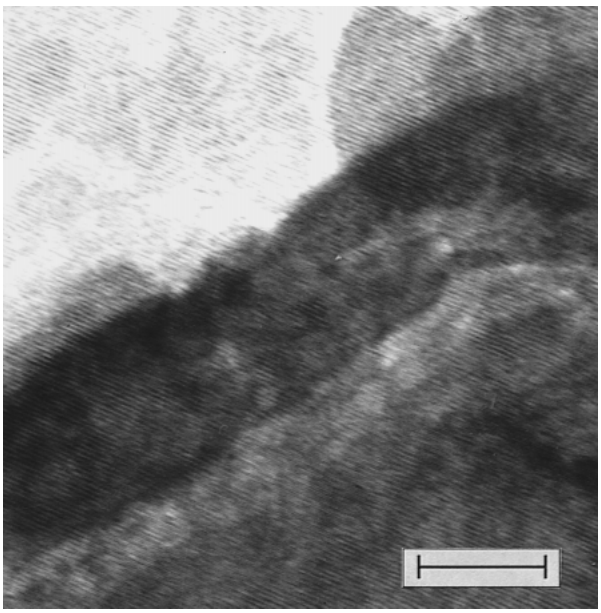

FIGURE 4. A TEM image of parascorodite reveals regular lattice fringes; scale bar corresponds to 59 nm.

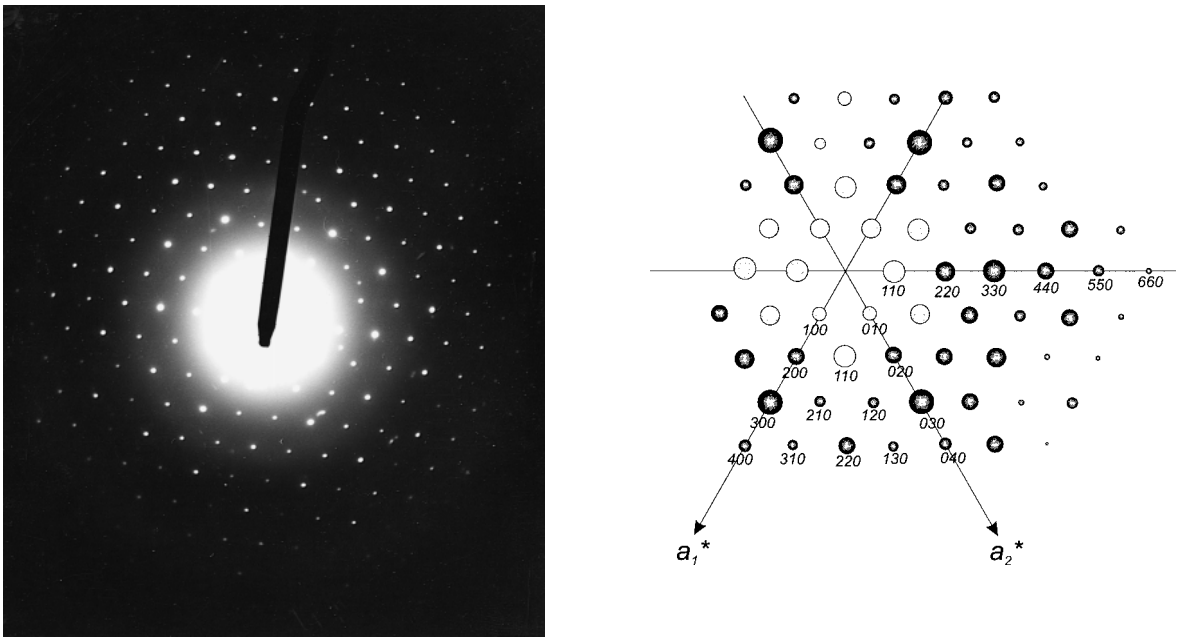

FIGURE 5. Electron-diffraction pattern of parascorodite (*hk*0), indicating hexagonal (trigonal) symmetry.

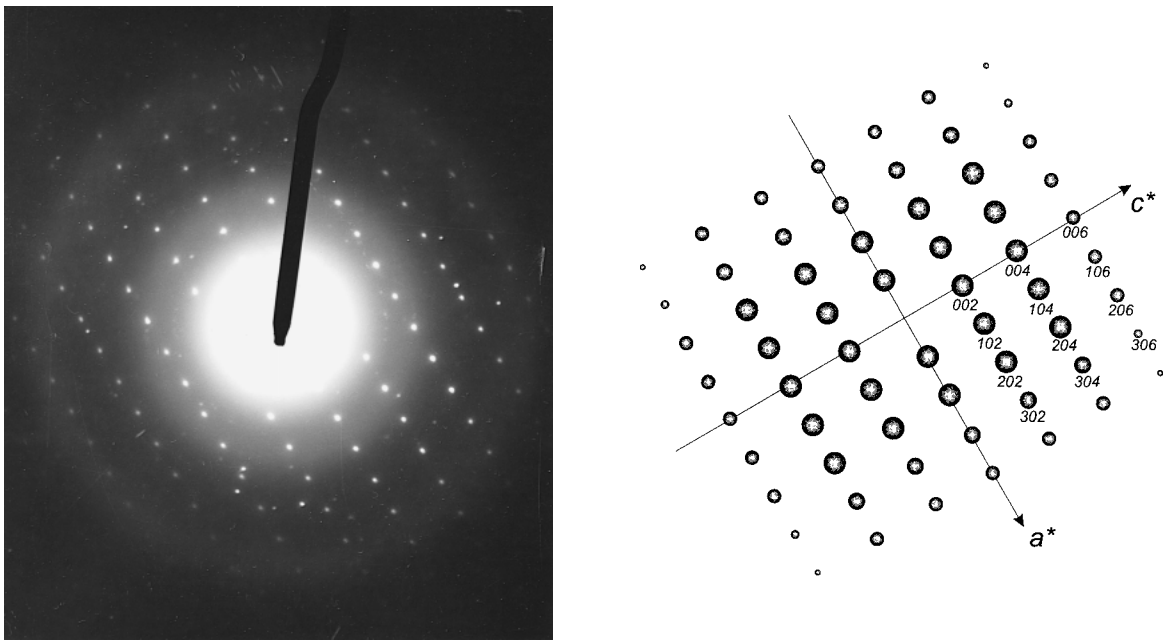

FIGURE 6. Electron-diffraction pattern of parascorodite (*h*0*l*) showing diffraction aspect *P*-*c*-.

irregular, slightly rounded boundaries (Fig. 2). Crystal size varies with prismatic crystals being up to 0.5 μm; rarely, also grains up to 1 μm have been observed. The high-resolution image (280 000×) reveals regular lattice fringes, indicating the crystalline character of the mineral (Fig. 4).

The electron diffraction pattern of (*hk*0) reciprocal lattice (Fig. 5) indicates hexagonal or trigonal symmetry and $a = b$ is 8.8–8.9 Å, which corresponds closely to the data refined from the X-ray powder diffraction pattern. The pattern (*h*0*l*) (Fig. 6) shows systematic absences resulting in extinction aspect *P*-*c*- with possible space groups: *P*3*c*1, $P\bar{3}c1$, $P6_3cm$, $P\bar{6}c2$, $P6_3/mcm$. Due to a thickness of prismatic parascorodite crystal, (*hhl*) and (*h*0*l*) diffraction patterns were more difficult to obtain and could have been also affected by dynamic effects. Diffraction

TABLE 2. X-ray powder diffraction pattern of parascorodite from Kaňk

I_{rel}	d_{obs} (Å)	d_{calc} (Å)	h	k	l
29	7.741	7.742	1	0	0
61	4.973	4.972	0	0	2
34	4.468	4.468	1	1	0
44	4.184	4.183	1	0	2
100	4.076	4.076	1	1	1
20	3.868	3.869	2	0	0
23	3.323	3.323	1	1	2
67	3.053	3.053	2	0	2
8	2.924	2.925	2	1	0
68	2.806	2.806	2	1	1
59	2.661	2.662	1	1	3
36	2.579	2.579	3	0	0
54	2.520	2.521	2	1	2
23	2.4847	2.4853	0	0	4
5	2.3659	2.3662	1	0	4
44	2.2891	2.2893	3	0	2
10	2.1924	2.1927	2	1	3
12	2.1456	2.1460	3	1	0
18	2.0973	2.0976	3	1	1
22	2.0903	2.0910	2	0	4
5	2.0366	2.0373	2	2	2
10	1.9697	1.9701	3	1	2
19	1.9339	1.9343	4	0	0
32	1.8935	1.8937	2	1	4
15	1.8160	1.8163	1	1	5
26	1.8019	1.8026	4	0	2
31	1.7892	1.7895	3	0	4
3	1.7742	1.7750	3	2	0
20	1.7472	1.7474	3	2	1
29	1.6881	1.6883	4	1	0
32	1.6713	1.6716	3	2	2
17	1.6440	1.6441	2	1	5
31	1.6239	1.6241	3	1	4
23	1.5645	1.5646	3	2	3
18	1.5531	1.5533	1	1	6
22	1.5264	1.5264	4	0	4
9	1.5227	1.5229	2	0	6
7	1.5040	1.5043	4	1	3
9	1.4887	1.4889	3	3	0
8	1.4847	1.4850	2	2	5
9	1.4771	1.4774	5	0	2
10	1.4445	1.4443	3	2	4
7	1.4413	1.4414	2	1	6
13	1.4026	1.4027	4	2	2
6	1.3894	1.3896	5	1	0
24	1.3761	1.3762	5	1	1
4	1.3581	1.3581	3	3	3
9	1.3531	1.3533	1	1	7

TABLE 3. Comparison of IR spectra of parascorodite and scorodite

Parascorodite, Kaňk		Scorodite, Djebel Debar, Algeria		Tentative assignment
ν [cm^{-1}]	I	ν [cm^{-1}]	I	
3510	w, b	3516	s	OH stretching
–*	–	~3300	s, b	H_2O stretching
3025	s, b	2969	m	see text
1620	m	1619	m, b	bending vibration of H_2O molecules
1040	w	1053	m	stretching vibration of $(PO_4)^{3-}$
1010	w	1022	m	stretching vibration of $(PO_4)^{3-}$
890	m, sh	–	–	stretching vibrations† of $(AsO_4)^{3-}$
840	vs	825	vs	stretching vibrations† of $(AsO_4)^{3-}$
800	vs	–	–	stretching vibrations† of $(AsO_4)^{3-}$
–	–	620	m, sh	vibration of Fe-OH_2
538	m	580	m, sh	vibration of Fe-OH_2
460	m	467	s	stretching vibrations† of $(AsO_4)^{2-}$
–	–	436	s	stretching vibrations† of $(AsO_4)^{2-}$
355	w, sh	–	–	probably cation translations
325	vw	–	–	probably cation translations
290	vw	–	–	probably cation translations

Notes: vs = very strong, s = strong, m = medium, w = weak, vw = very weak, character of absorption maxima: sh = shoulder, b = broad.
* Poorly resolved.
† Degeneracies are removed by low crystal symmetry.

spots are intense and sharp indicating well-ordered, defect-free crystals.

Infrared spectra

Infrared transmission spectra were recorded with a Perkin-Elmer 325 spectrophotometer using KBr pellets in the range 180–4000 cm^{-1}. The IR spectra of parascorodite from Kank and scorodite from Djebel Debar (Algeria) (Fig. 7) exhibit typical arsenate and phosphate IR bands (assigned in Table 3). The difference in mid-IR peak widths are probably due to grain size (e.g., Hofmeister 1995) as parascordite is uniformly very fine grained.

The high frequency regions of the two minerals differ considerably. Scorodite has a broad band centered near 3300 cm^{-1} which is due to molecular H_2O with two superimposed sharp peaks. The relatively sharp 3516 cm^{-1} band is undoubtably OH, but the sharp 2969 cm^{-1} could be either organic contamination

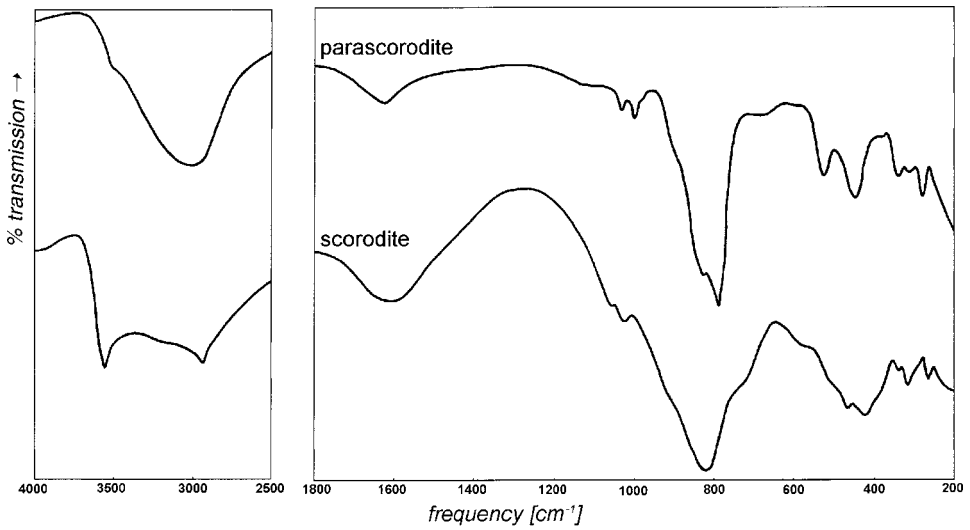

FIGURE 7. Infrared transmission spectra of parascorodite from Kaňk and scorodite from Djebel Debar (Algeria).

or OH with some hydrogen bonding. Parascorodite also has the sharp OH band at 3510 cm^{-1}. This region is dominated by a broad band at 3025 cm^{-1}, which must be underlain by H_2O absorptions, because an H_2O band is seen at 1620 cm^{-1} (Table 3, Fig. 7). The 3025 cm^{-1} band might be OH^-, but if so, this environment has a variable degree of hydrogen bonding and differs considerably from scorodite.

ACKNOWLEDGMENTS

Recent study of secondary minerals from the Jáchymov ore district confirming parascorodite from a second locality was supported by the Grant Agency of the Czech Republic projects nos. 205/93/0900 and 205/97/0491.

REFERENCES CITED

Čech, F., Jansa, J., and Novák, F. (1976) Kaňkite, $FeAsO_4.3H_2O$, a new mineral. Neues Jahrbuch für Mineralogie, Monatshefte, 1976, 426–436.

Čech, F., Jansa, J., and Novák, F. (1978) Zýkaite, $Fe_4^{3+}(AsO_4)_3(SO_4)(OH).15H_2O$, a new mineral. Neues Jahrbuch für Mineralogie, Monatshefte, 1978, H. 3, 134–144.

d'Yvoire, F. and Ronis, M.C.R. (1968) Sur le polymorphisme de $FeAsO_4$. Academie des Sciences Paris, Comptes Rendues Hebdomaires Séances, Série. C 267, 955–958.

Novák, F., Povondra, P., and Vtělenský, J. (1967) Bukovskýit, $Fe_2^{3+}(AsO_4)(SO_4)(OH).7H_2O$, from Kaňk, near Kutná Hora a new mineral. Acta Universitatis Carolinae, Geologica, 1967, 297–325.

Ondruš, P., Veselovský, F., and Hloušek, J. (1997a) A review of mineral associations and paragenetic groups of secondary minerals of the Jáchymov (Joachimsthal) ore district. Journal of the Czech Geological Society, 42, 4, 109–115.

Ondruš, P., Veselovský, F., Hloušek, J., Skála, R., Vavřín, I., Frýda, J., Čejka, J., and Gabašová, A. (1997b) Secondary minerals of the Jáchymov (Joachimsthal) ore district. Journal of the Czech Geological Society, 42, 4, 3–76.

Ondruš, P., Veselovský, F., Skála, R., Císařová, I., Hloušek, J., Frýda, J., Vavřín, I., Čejka, J., and Gabašová, A. (1997c) New naturally occurring phases of secondary origin from Jáchymov (Joachimsthal). Journal of the Czech Geological Society, 42, 4, 77–108.

Trdlička, Z. and Hoffman, V. (1965) Skorodit von Kutná Hora (Kuttenberg), Tschechoslowakei. Chemie der Erde, 24, 223–229.

MANUSCRIPT RECEIVED MAY 28, 1998
MANUSCRIPT ACCEPTED APRIL 15, 1999
PAPER HANDLED BY GILBERTO ARTIOLI